Adıyaman University Journal of Science
https://dergipark.org.tr/en/pub/adyujsci
DergiPark AKADEMİK
ISSN 2147-1630
e-ISSN 2146-586X

Molecular Docking and ADMET Profiling Studies of some Fluorinated Sulfonates and their Schiff Base Derivatives: Potential inhibitors of HMG-CoA Reductase

Selami ERCAN[1,*]

[1]*Batman University, Faculty of Arts and Sciences, Department of Chemistry, 72000, Batman, Türkiye*
selami.ercan@batman.edu.tr, ORCID: 0000-0002-9528-6122

Received: 30.06..2025 **Accepted:** 14.12.2025 **Published:** 31.12.2025

Abstract

Hypercholesterolemia is one of the major risk factors of cardiovascular diseases. HMG-CoA reductase enzyme, the main drug target to reduce the cholesterol levels, catalyzes biosynthesis of cholesterol. In addition to *in-silico* estimations of ADMET profiles of compounds composed of several functional groups which are known to be effective for many diseases, a molecular docking study was performed to investigate binding modes of compounds in binding site of HMG-CoA reductase. Prior to docking studies, the RESP charges of compounds were defined by quantum mechanics calculations. Analyzes revealed that eleven Schiff base derivatives showed better binding rather than co-crystallized drug Rosuvastatin. Results demonstrated that Schiff base group included compounds have better inhibition effects on HMG-CoA reductase than their related pre-compounds. The docking scores of compounds range between -7.22 kcal/mol and -9.43 kcal/mol. The compounds L16, L28, and L15 were the ligands having best binding scores with the values -9.43 kcal/mol, -9.24 kcal/mol, and -9.23 kcal/mol, respectively. The analyses showed that compounds interact with several key residues of enzyme such as Glu559, Asp690, Lys691, Lys692, and Asp767.

Keywords: Aryl sulfonates; Schiff bases; HMG-CoA reductase; ADMET; Molecular docking.

* Corresponding Author DOI: 10.37094/adyujsci.1730312

Bazı Florlu Sülfonatların ve Schiff Baz Türevlerinin Moleküler Yerleştirme ve ADMET Profilleme Çalışmaları: HMG-CoA Redüktazın Potansiyel İnhibitörleri

Öz

Hiperkolesterolemi, kardiyovasküler hastalıkların başlıca risk faktörlerinden biridir. Kolesterol seviyelerini düşürmek için ana ilaç hedefi olan HMG-CoA redüktaz enzimi, kolesterolün biyosentezini katalize eder. Birçok hastalık için etkili olduğu bilinen çeşitli fonksiyonel gruplardan oluşan bileşiklerin ADMET profillerinin in silico tahminlerine ek olarak, HMG-CoA redüktazın bağlanma bölgesindeki bileşiklerin bağlanma modlarını araştırmak için moleküler yerleştirme çalışması yapıldı. Yerleştirme çalışmalarından önce, bileşiklerin RESP yükleri kuantum mekaniği hesaplamalarıyla tanımlandı. Analizler, on bir Schiff bazı türevinin ko-kristalize ilaç Rosuvastatin'den daha iyi bağlanma gösterdiğini ortaya koydu. Sonuçlar, Schiff bazı grubu içeren bileşiklerin, ilgili ön bileşiklere göre HMG-CoA redüktaz üzerinde daha iyi inhibisyon etkilerine sahip olduğunu gösterdi. Bileşiklerin yerleştirme puanları -7,22 kcal/mol ile -9,43 kcal/mol arasında değişmektedir. L16, L28 ve L15 bileşikleri sırasıyla -9,43 kcal/mol, -9,24 kcal/mol ve -9,23 kcal/mol değerleriyle en iyi bağlanma skorlarına sahip ligandlardı. Analizler bileşiklerin Glu559, Asp690, Lys691, Lys692 ve Asp767 gibi enzimin birkaç önemli kalıntısıyla etkileşime girdiğini gösterdi.

Anahtar Kelimeler: Aril sülfonatlar; Schiff bazları; HMG-CoA redüktaz; ADMET; Moleküler yerleştirme.

1. Introduction

Cardiovascular disease (CVD), cancer, chronic respiratory disease, and diabetes are the four main noncommunicable diseases (NCD) causing death. Hypertension and hypercholesterolemia are the significant risk factors of CVD diseases [1]. Hypercholesterolemia caused by cholesterol which derived from acetyl-CoA on the mevalonate pathway [2]. The synthesis of cholesterol could be prevented by inhibition of a key enzyme 3-Hydroxy-3-methylglutaryl-CoA (HMG-CoA) reductase (HMGR). Inhibition of HMGR results with ending of the conversion of the HMG-CoA to mevalonate and synthesis of subsequent products. The studies revealed that termination of this path can cause growth arrest and cell death in cells of several cancer types [3-7]. Statins are the most popular inhibitors used to inhibit HMGR which are derived from fungal metabolites or from microbial sources [8]. Despite showing great success in inhibition of HMGR and lowering the levels of low-density lipoprotein, the researches

demonstrated that high dosages of statins required to lower the LDL-C to the levels (70 mg/dL) preferred by U.S. Cholesterol Education Program may can cause myalgia [9].

Consisting of 888 residues, HMGR could be investigated in three domains: membrane anchor domain (1-339 residues), linker domain (340-459 residues), and catalytic domain (460-888 residues). The catalytic domain of HMGR structurally divided in three subdomains: N-terminal as N-domain, a large domain as L-domain and a small domain as S-domain. The smallest domain, N terminal domain, includes residues 460-527 and connects catalytic portion of HMGR to the membrane domain[6]. The central L-domain (528-590) has an ENVIG dimerization motif [10]. The S-domain (592-682) of catalytic domain includes DAMGMN NAD(P) binding motif[10] and is inserted between Lβ3 and Lα2 of L-domain [6]. The S-domain connects to the L-domain through β-strand (Lβ3 and Sβ1) and the cis-loop (residues 682-694) which is essential for HMG-binding site [6].

To date, many studies including *in* vitro and/or *in* silico methods have been performed to inhibit HMGR using statin derivatives [10, 11], non-statins [12, 13] and natural sources [14-16] based compounds as inhibitor candidates. In the current study we aimed to introduce new inhibitors having pyrazolone, Schiff base, aryl sulfonate, and fluorine substituted compounds to the inhibition efforts of HMGR. In addition to antimicrobial, antitumor, central nervous system (CNS) activity, antioxidant, anti-tubercular, antiviral, lipid-lowering, antihyperglycemic and protein inhibitory activities of pyrazolone [17], it was also reported to be included in amyotrophic lateral sclerosis [18], anti-inflammatory [19], idiopathic chronic immune thrombocytopenia[20], and pain [21] drugs. Sulfonate group functional group possess diverse bioactive properties, including antibacterial, antiviral, anticancer, and anti-inflammatory activities [22, 23]. Schiff bases were reported to include anti-diabetic, tumor-preventative, anti-proliferative, cancer-preventative, anticorrosive, and anti-inflammatory effects [24-28].

Computer aided drug design techniques have been widely used in drug design and development processes [29, 30] and have been reported to decrease the cost of drug development process up to 50 [31]. The druggability properties of a drug candidate is a crucial issue [32] where it depends on absorption, distribution, metabolism, extraction and toxicity (ADMET) properties of a molecule. Nevertheless, molecular docking is one of the fast and economic method [33] in CADD processes which is a structure-based drug design method and needs 3D structure of the target molecule. The method predicts the binding affinity of the drug against a drug target [34].

Some crystal structures of HMG-CoA reductase enzyme complexed with HMG-CoA in addition to various ligands, such as atorvastatin, simvastatin, fluvastatin, and rosuvastatin (RSV)

have hitherto been resolved [6, 35-37]. RSV has been reported as the most effective inhibitor among statin group inhibitors [38-40]. Hence, we have used a crystal structure of enzyme complexed with RSV in the current study to compare the docking results of the newly studied ligands. The compounds used in the current study were synthesized and characterized formerly (Scheme 1) [41]. The study includes ADMET properties of the synthesized compounds in addition to their molecular docking studies in the binding site of HMG-CoA reductase enzyme structure.

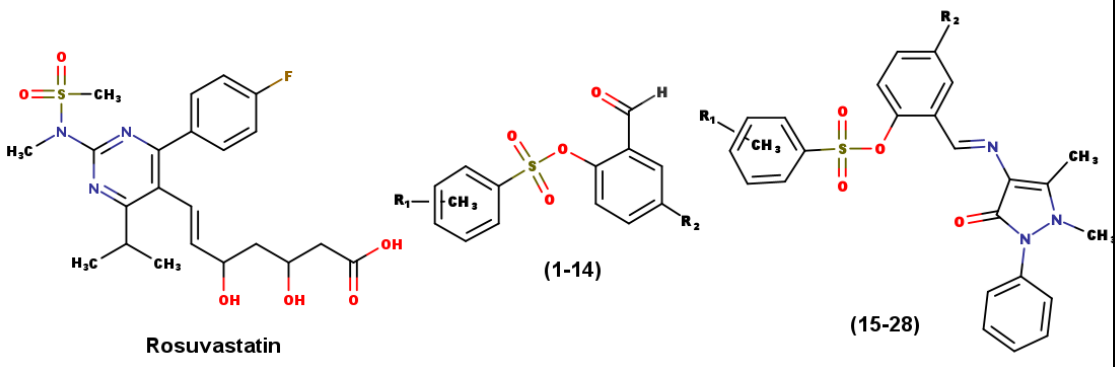

Molecules		R_1	R_2	Molecules		R_1	R_2
L01	**L15**	3-CF_3	H	**L08**	**L22**	4-CF_3	H
L02	**L16**	3-CF_3	F	**L09**	**L23**	4-CF_3	F
L03	**L17**	3-CF_3	Cl	**L10**	**L24**	4-CF_3	Cl
L04	**L18**	3-CF_3	Br	**L11**	**L25**	4-CF_3	Br
L05	**L19**	3-CF_3	CH_3	**L12**	**L26**	4-CF_3	CH_3
L06	**L20**	3-CF_3	OCH_3	**L13**	**L27**	4-CF_3	OCH_3
L07	**L21**	3-CF_3	NO_2	**L14**	**L28**	4-CF_3	NO_2

Scheme 1: The 2D representations of fluorinated sulfonates (1-14), their Schiff base derivatives (15-28) [41] and co-crystallized Rosuvastatin.

2. Materials and Methods

2.1. ADMET Studies

The ADMET studies of the compounds were performed via SwissADME (**http://www.swissadme.ch/**) [42] and pkCSM pharmacokinetics (**https://biosig.lab.uq.edu.au/pkcsm/**) [43] web servers. Simplified molecular-input line entry specification (SMILES) nomenclature of ligands were used to calculate ADMET descirptors.

2.2. Ligand and Receptor Preparation and Molecular Docking

The crystal structure of HMGR was obtained from protein databank (www.rcsb.org) with the code of 1HWL [35] complexed with RSV inhibitor. The structures of protein and RSV were saved separately by removing all unnecessary particles. The optimized structures of studied

ligands [41] were obtained from one of our previous studies. RESP charges [44] of all studied ligands were calculated to produce more accurate results. Chimera and MGL Tools programs were utilized in preparation of the structures for the docking process. The ligands were divided in two classes due to their structural skeletons since ligands 1-14 doesn't contain Schiff base group.

The docking studies were performed by Autodock Vina (v1.2.7) [45], a fast and user-friendly docking engine. The docking region was defined by centering a grid box on the co-crystallized RSV ligand with the dimensions of 21 Å, 31 Å, and 20 Å and with the coordinates of 21.32, -31.23, 27.05 through x, y, and z orientations, respectively. Nine docking poses were produced for each molecule.

Prior to docking studies, a validation test was performed by re-docking of RSV to the binding site of enzyme.

3. Results and Discussion

3.1. ADMET Properties of the Compounds

ADMET properties of the chemicals could be estimated on the basis of the structural properties of compounds, [46, 47] where theoretical methods have been applied efficiently in recent years [48, 49]. The ADMET properties of the studied compounds were predicted using SwissADME and pkCSM web servers. There are several drug-likeness methods defined by Lipinski [50, 51], Ghose [52], Veber [53], Egan [54], and Muegge [55]. The Lipinski's [50, 51] rule of five states that a drug candidate should meet the following criteria: molecular weight (MW) ≤ 500Da, calculated LogP (cLogP) ≤ 5 and ≥0, hydrogen bond donors (HBD) ≤ 5, hydrogen bond acceptors (HBA) ≤ 10, and polar surface area (PSA) ≤ 140 $Å^2$. Nevertheless, there are some differences in the ranges of the properties in the other methods. Moreover, Muegge's [55] method involves numbers of cyclic rings, carbon atoms, heteroatoms, and rotational bonds rules. The physicochemical parameters of the studied ligands and co-crystallized RSV predicted by SwissADME and results are summarized in Table 1. While the violations demonstrated by ligands in accordance with Lipinski's rule of five represented here the results of other methods have been given in Supporting Information Table 1. The results revealed that the molecular weights of the ligands range from 330.28 Da to 594.40 Da where the compounds having a molecular weight more than 500 Da represents a violation as to Lipinski's rule. Since the compounds do not include any hydrogens attached to the electronegative atoms such as oxygen and nitrogen the numbers of hydrogen bond donors are 0 for L01-L28, while RSV has 3 hydrogen bond donors. In addition, all the ligands meet the criterion of having less than or equal to 10 numbers of hydrogen bond acceptor. The polar surface areas of the compounds change between 68.82 $Å^2$ and 149.30 $Å^2$,

where only RSV have a value more than 140 Å^2. The LogP descriptor is the partition coefficient of a molecule between n-octanol and water which is related to the lipophilicity of the molecule [56, 57]. SwissADME calculates consensus $LogP_{o/w}$ descriptor, which is an arithmetic mean of the iLogP, XlogP3, WlogP, MLogP and Silicos-IT descriptors. Additionally, the results showed that L15-L20 and L22-L27 ligands do not meet the criterion of LogP value.

Table 1: Physicochemical parameters of studied compounds predicted by SwissADME tool

Mol	MW (g/mol)	HBA[a]	HBD[b]	MR[c]	PSA[d] (Å^2)	C.LogP[e] ($P_{o/w}$)	Lipinski Violations
L01	330.28	7	0	71.13	68.82	3.54	0
L02	348.27	8	0	71.09	68.82	3.83	0
L03	364.72	7	0	76.14	68.82	3.99	0
L04	409.18	7	0	78.83	68.82	4.08	0
L05	344.31	7	0	76.10	68.82	3.84	0
L06	360.31	8	0	77.62	78.05	3.49	0
L07	375.28	9	0	79.95	114.64	2.84	0
L08	330.28	7	0	71.13	68.82	3.57	0
L09	348.27	8	0	71.09	68.82	3.83	0
L10	364.72	7	0	76.14	68.82	3.99	0
L11	409.18	7	0	78.83	68.82	4.09	0
L12	344.31	7	0	76.10	68.82	3.86	0
L13	360.31	8	0	77.62	78.05	3.51	0
L14	375.28	9	0	79.95	114.64	2.91	0
L15	515.50	8	0	129.25	91.04	5.09	2
L16	533.49	9	0	129.21	91.04	5.44	2
L17	549.95	8	0	134.26	91.04	5.66	2
L18	594.40	8	0	136.95	91.04	5.71	2
L19	529.53	8	0	134.22	91.04	5.42	2
L20	545.53	9	0	135.75	100.27	5.11	1
L21	560.50	10	0	138.08	136.86	4.52	1
L22	515.50	8	0	129.25	91.04	5.12	2
L23	533.49	9	0	129.21	91.04	5.42	2
L24	549.95	8	0	134.26	91.04	5.64	2
L25	594.40	8	0	136.95	91.04	5.70	2
L26	529.53	8	0	134.22	91.04	5.42	2
L27	545.53	9	0	135.75	100.27	5.16	1
L28	560.50	10	0	138.08	136.86	4.51	1
RSV	481.54	9	3	123.40	149.30	2.25	0

[a]Hydrogen bond acceptor, [b]Hydrogen bond donor, [c]Molar refractivity, [d]Polar surface area, [e]Consensus LogP

The absorption, distribution, metabolism, excretion and toxicity properties of a molecule have substantial role in drug-likeness of the molecule. Absorption, the movement of a drug from an extravascular site of administration into the systemic circulation [56, 57], can be predicted by

solubility, lipophilicity (given above) and intestinal absorption in human descriptors of a molecule. The SwissADME tool considers the compounds representing more negative values than -6 as poorly soluble. Hereunder, L01-L14 ligands predicted to be as moderately soluble, L15-L28 ligands are poorly soluble and RSV is predicted as soluble. The intestinal absorption in human descriptors were predicted by pkCSM and plotted in Fig. 1. While most of the ligands showed to have values more than 87%, the ligand L28 has the worst intestinal absorption percent in human with the 42.23% value and RSV followed it with a value of 44.88%.

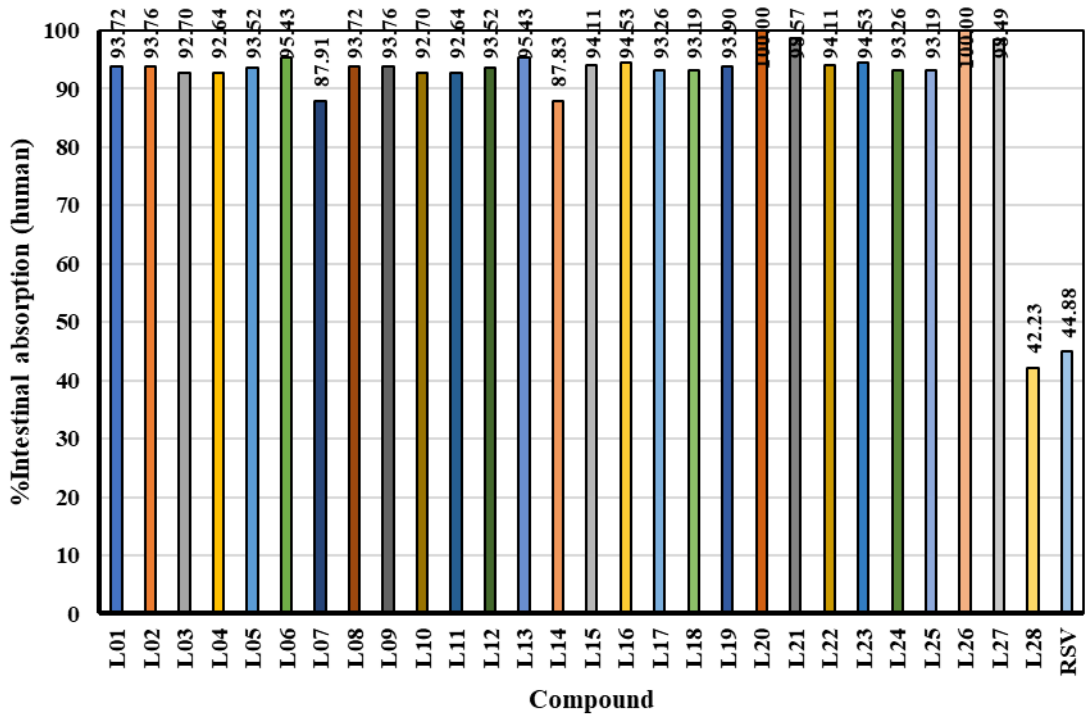

Figure 1: Predicted intestinal absorption (human) values of the compounds used in the study

Distribution properties of the molecules were predicted by SwissADME and pkCSM using descriptors glycoprotein P (P-gp) substrate, blood-brain barrier (BBB) permeability and fraction unbound. Among the compounds only L28 and RSV were predicted to be P-gp substrate. BBB regulates the transfer of cells, nutrients and materials included in blood to the brain and vice versa to maintain homeostasis in the central nervous system (CNS) [58, 59]. The BBB permeabilities of the studied ligands were predicted in the range of -1.96 to 0.28 according to pkCSM (SI Table S2), where the results were given as permeable or not by SwissADME, all the compounds have been defined as non-permeant to CNS. Fraction unbound is the descriptor attributed to the amount of the drug ruptured from serum proteins. The fraction unbound effects glomerular filtration, hepatic metabolism, volume of distribution, and total clearance [59, 60]. Moreover, the fraction unbound represents the amount of the drug in action. The fraction unbound values of the

compounds are in the range of 0-0.251. Where the L07 and L14 ligands were predicted to have 0 fraction unbound, L16 ligand demonstrated the highest fraction unbound (SI Table S2).

The metabolism of drugs is another important issue in the drug development process, which includes the biotransformation of molecules. Among the reported enzymatic reactions CYPs are the most included enzymes with a value of more than 90% [61, 62]. Cytochrome P450 enzymes are mostly assigned to the metabolism process in the liver and intestine. CYP1A2, CYP2C19, CYP2C9, CYP2D6 and CYP3A4 are types of the P450 enzyme family [59]. The predicted inhibitor and substrate properties of the compounds against CYPs are defined by pkCSM are given in Supporting Information Table X. The results have demonstrated that where only L28 may have substrate effect for CY2D6 enzyme, all the compounds may act as substrate for CYP3A4 enzyme. Additionally, the numbers of the compounds those may show inhibition effects for CYP1A2, CYP2C19, CYP2C9, CYP2D6, and CYP3A4 enzymes are 6, 27, 23, 0, and 13, respectively (SI Table S2).

Excretion is the last step of pharmacokinetics. It primarily consists of hepatic and renal clearance which called total clearance as the sum of two clearance types. Since bioavailability and half-life of drugs have been affected by clearance [63], it can be used for dosing sizes of drugs [43, 59]. The pkCSM pharmacokinetics tool predicted the total clearance values of the compounds in a range of -0.33 ml/min/kg to 1.32 ml/min/kg. The results can be evaluated as high clearance for values greater than or equal to 0.7 ml/min/kg, low clearance for the values lower than or equal to 0.3 ml/min/kg, and fair clearance for the values between 0.3 ml/min/kg and 0.7 ml/min/kg (SI Table S2).

The hepatotoxicity, AMES toxicity, and the human ether-a-go-go related gene (hERG) I and II inhibitory preferences of the compounds were predicted by pkCSM pharmacokinetics, as well, to determine toxicity levels of the compounds. All the ligands were predicted to be hepatotoxic according to results. The ligands L01-L03, L05-L10, L12-L14, L21, and L22 were predicted to have AMES toxicity properties. In addition, where none of the ligands have been predicted as hERG I inhibitor, L15-L27 ligands were predicted to have inhibitory effect for hERG II enzyme (SI Table S2).

3.2. Molecular Docking Studies of the Compounds

The co-crystallized ligand, RSV was re-docked to the binding site of the HMG-CoA reductase enzyme do validate the docking methodology. The method was validated by obtaining an RMSD of 1.182 Å between re-docked and co-crystallized structures of the ligand (Fig. 2.).

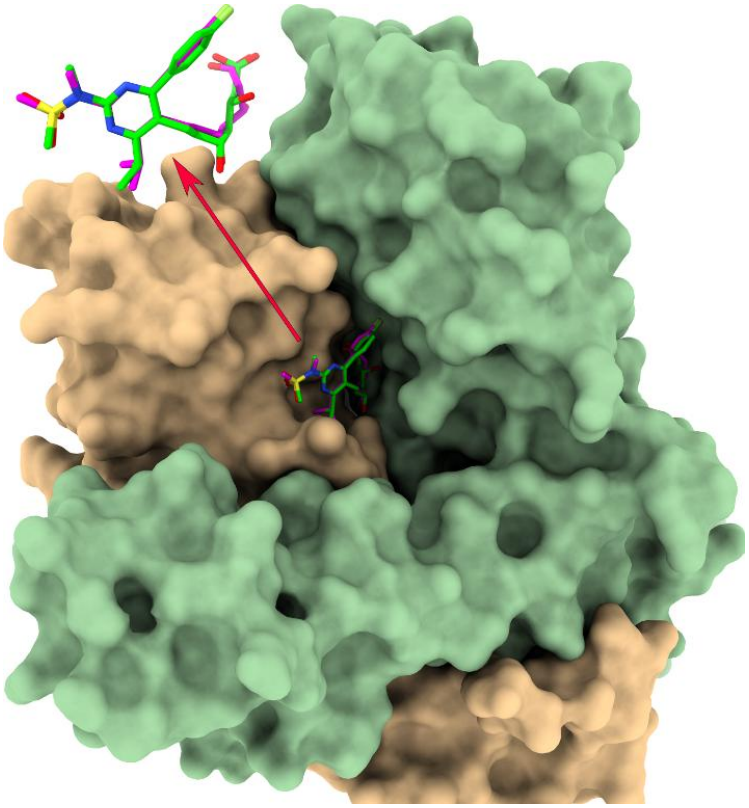

Figure 2: Binding modes of co-crystallized RSV and its re-docked structure in binding site of enzyme (Chain C: dark sea green, Chain D: burly wood). The carbon atoms of co-crystallized structure and re-docked structure are given as green and magenta, respectively.

Molecular docking studies of the ligands were performed following validation process. The binding poses of the ligands were depicted in Fig. 3. Since the docking studies were performed with ligands having RESP charges, we have optimized RSV and thus RESP charges added RSV structure was also docked to binding site of enzyme and the RMSD value between the RESP charged RSV and co-crystallized RSV was 1.221 Å.

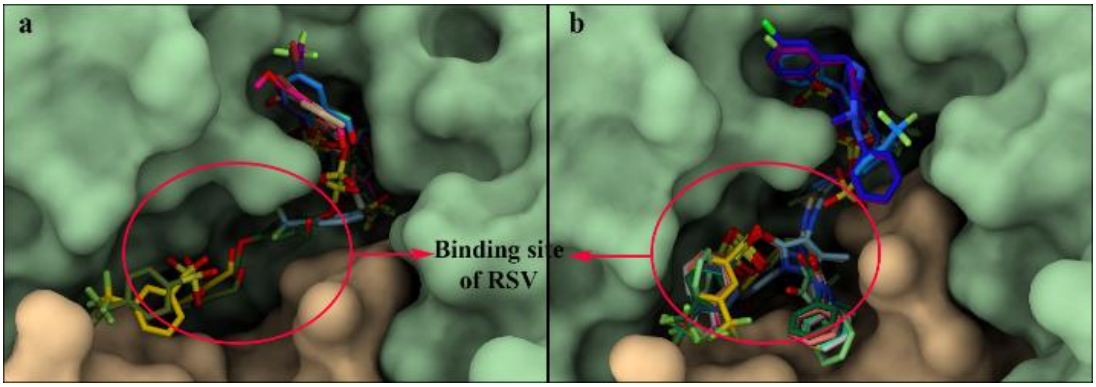

Figure 3: Binding modes of fluorinated sulfonates (1-14) (**a**), their Schiff base derivatives (15-28) (**b**) in the binding site of HMGR enzyme (Chain C: dark sea green, Chain D: burly wood)

Following the validation of the docking method, all studied compounds were docked to the binding site of the HMG-CoA reductase enzyme. The results demonstrated that nine newly

studied compounds have better docking scores than RSV docked with RESP charges, and ten of the compounds showed better binding scores than co-crystallized RSV used with Gasteiger charges. The docking scores of the compounds are in the range of -7.22 kcal/mol and -9.43 kcal/mol (Table 2). It was observed that the compounds coded as **L15-L28** showed better binding properties (-7.93 kcal - -9.35 kcal/mol) to the binding site of HMG-CoA reductase enzyme than of compounds coded as **L01-L14** (-7.22 kcal/mol - -7.79 kcal/mol). Among the compounds, compound coded as **L16** has the best binding free energy value with the -9.43 kcal/mol. Where L01-L06, L08-L13, L22, L23, and L24 did not locate into the binding site of enzyme as RSV did, L15 and L16 placed partly, and other compounds settled in completely (Fig. 3). Furthermore, we have discussed here the ligand-residue interactions of three best scored compounds (compounds having scores lower than -9.00 kcal/mol) and 2D interactions maps of remaining compounds were given in Supporting Information (Fig. S1-S25).

Table 2: Docking scores of studied compounds.

Compounds	Scores (kcal/mol)	Compounds	Scores (kcal/mol)
RSV[a]	**-8.44**	**L14**	-7.59
RSV[b]	**-8.50**	**L15**	**-9.23**
L01	-7.40	**L16**	**-9.43**
L02	-7.50	**L17**	-8.90
L03	-7.42	**L18**	-8.52
L04	-7.43	**L19**	-8.69
L05	-7.59	**L20**	-8.44
L06	-7.39	**L21**	-8.75
L07	-7.79	**L22**	-7.93
L08	-7.34	**L23**	-8.06
L09	-7.47	**L24**	-8.16
L10	-7.52	**L25**	-8.50
L11	-7.51	**L26**	-8.54
L12	-7.50	**L27**	-8.25
L13	-7.22	**L28**	**-9.24**

[a]Co-crystallized RSV docked with Gasteiger charges, used for validation of docking method,
[b]Optimized structure of RSV docked with RESP charges

Since the binding site of the enzyme is formed by a homodimer of the enzyme, the residues are given with C or D before residue names to define the chain of the residues. The co-crystal ligand RSV has seven hydrogen bonds with HMG-CoA reductase residues including C:Glu559, C:Arg590 (two bonds), C:Lys691, C:Lys692, D:Lys735, and Asn755 residues. The fluorine atom of the RSV creates two halogen interactions with C:Arg590 and C:Val683 residues. In addition to this, ligand has a pi-cation type interaction with C:Arg590 and two pi-alkyl interactions with D:Leu853 and D:Leu857 residues. The interactions of co-crystallized and re-docked structure of RSV are represented in Fig. 4 as 2D.

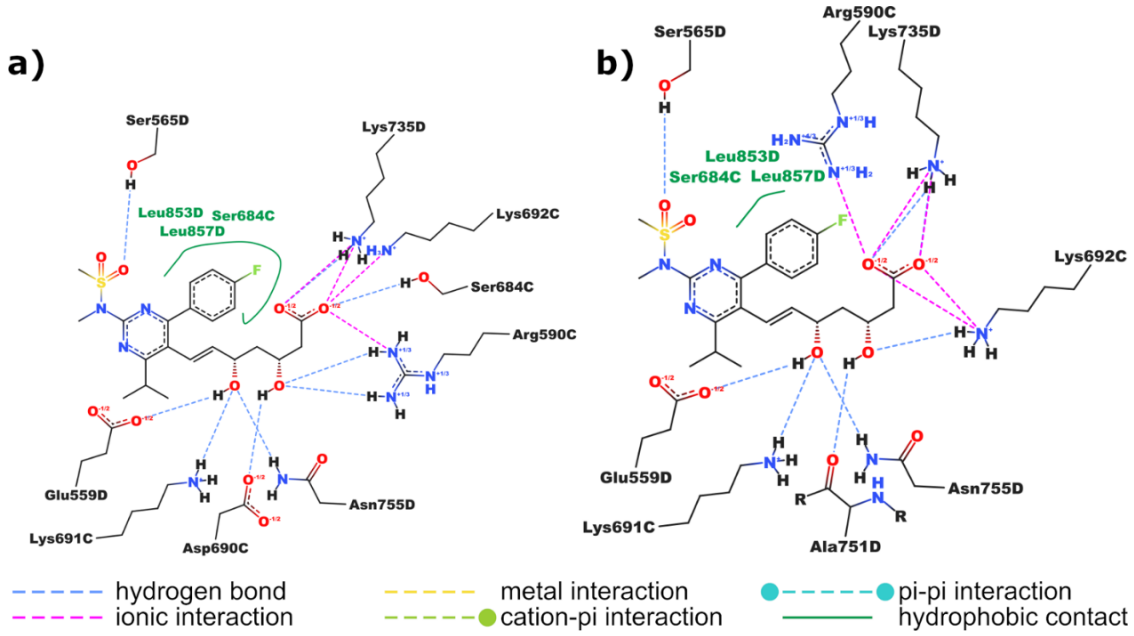

Figure 4: 2D representations of interactions of co-crystallized RSV ligand in the crystal structure of HMG-CoA enzyme (**a**), and interactions of re-docked RSV in the crystal structure of HMG-CoA enzyme (**b**)

Whereas Autodock Vina scores docking results of compounds as their binding free energy values, L15, L16 and L28 compounds showed the best binding free energy values with the scores of -9.23 kcal/mol, -9.43 kcal/mol, and -9.24 kcal/mol, respectively. L16, the compound which has best binding score, creates 1 conventional hydrogen bond via one of its fluorine atoms with HN atom of C:Asp767 residue. The compound demonstrates two halogen type interaction via two of its fluorine atoms with C:Asp690 and C:Gly765 residues. There is also a pi-cation interaction with C:Arg590, and two pi-anion interactions with residues C:Asp767 and D:Glu559. The compound demonstrates hydrophobic interactions with C:Cys561, C:Met655, C:Met657, and D:Leu853 residues (Fig. 5).

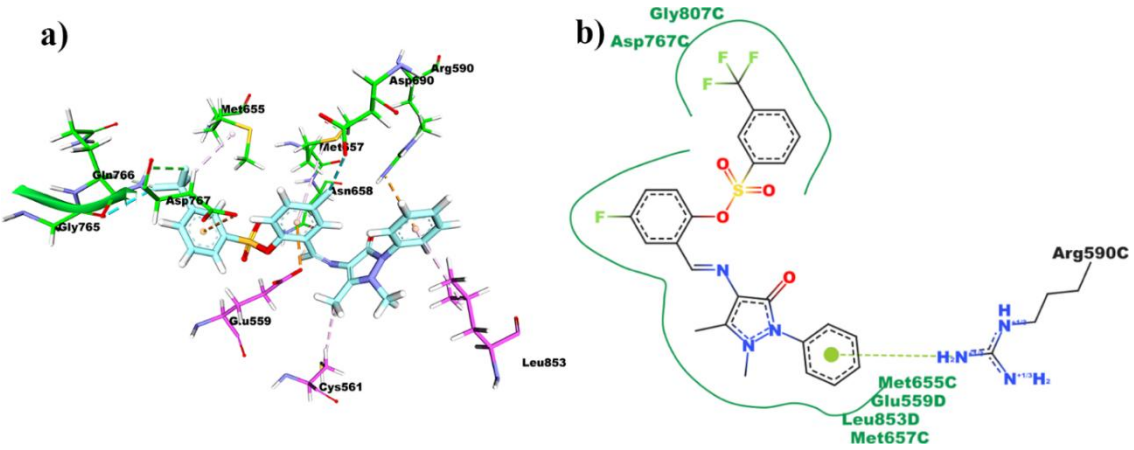

Figure 5: Interactions of L16 compound in binding site of HMG-CoA enzyme; **a)** 3D representation and **b)** 2D representation

The compound L28 was the second-best binding compound according to the docking results. Analyzing of the interactions showed that compound acts as a hydrogen bond acceptor with its oxygen atoms with C:Arg590 (two bonds), and D:Lys857 residues. In addition, fluorine atoms of the compound interact with C:Glu665, D:Ala856, D:Gly860 residues via halogen type interactions. The other interactions of the compound include, electrostatic pi-cation interaction with C:Arg590, and hydrophobic interactions with D:Leu853, C:Val683, D:His752, D:Leu857, DCys561, D:Ala856, and C:Val683 residues (Fig. 6).

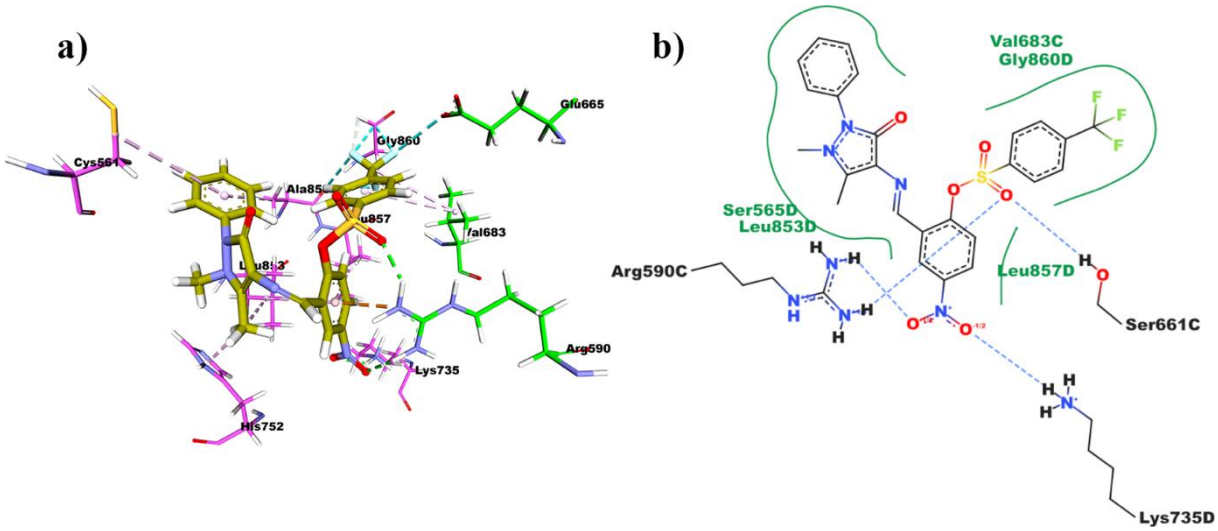

Figure 6: Interactions of L28 compound in binding site of HMG-CoA enzyme; **a)** 3D representation and **b)** 2D representation.

L15, the compound which has third best binding score, creates 4 conventional hydrogen bonds where two of them include hydrogen atoms of the enzyme residues and fluorine atoms of the compound. C:Arg590 (two hydrogen bonds), C:Asn658, and C:Asp767 residues of chain C of the enzyme. One of the fluorine atoms creates halogen type interactions with C:Gly765 and C:Gln766 residues. The compound has same pi-cation and pi-anion interactions as L16. The compound creates hydrophobic interactions with C:Met655, C:Met657, D:Leu853, and D:Leu857 residues (Fig. 7).

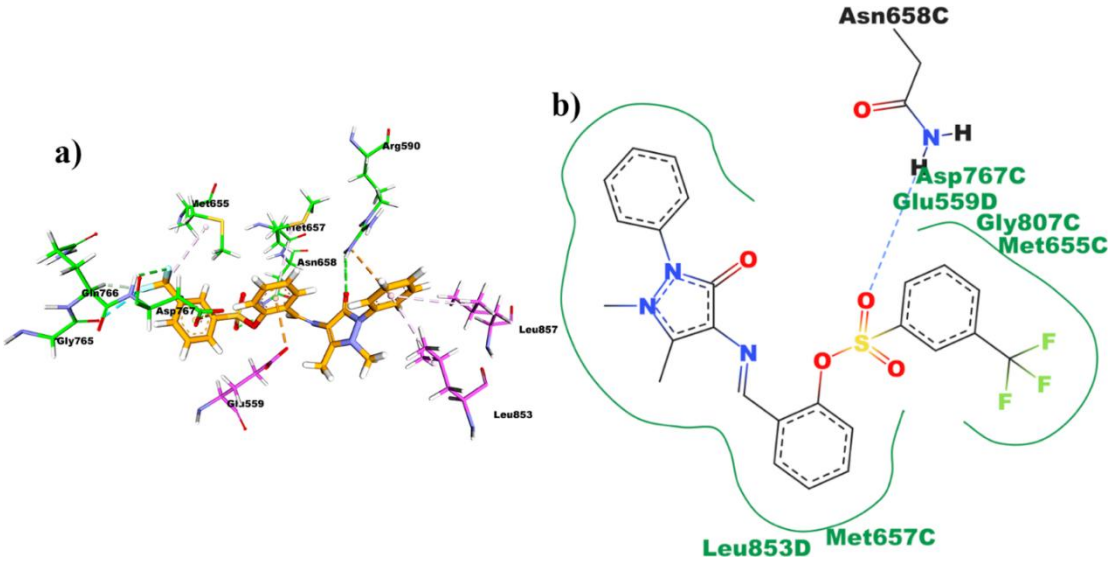

Figure 7: Interactions of L15 compound in binding site of HMG-CoA enzyme; **a)** 3D representation and **b)** 2D representation

The catalytic site of HMGR is located between the L- and the S-domain of the enzyme. The most crucial structural element of the binding site is the '*cis*-loop' (682-694 residues) bending trough the HMG. The position of the Asp690, Lys691, and Lys692 residues are provided by *cis*-peptide bond of Cys688 and Thr689 [6]. Glu559, Lys691 and His866 are the catalytic key residues [64, 65]. The docking results revealed that the all the compounds have contacts with Glu559 where none of them do not create interaction with neither Cys688 nor Thr689 residues. In addition, Istvan and co-workers [6] have proposed the residue Asp767 as crucial, since it was thought to form ionic interactions with Lys691 and thus stabilizing side chain of Lys691 in the active site. It was found that most of the studied compounds form interactions with this residue.

4. Conclusion

The ADMET profiles is a valuable tool for prediction of the pharmacological and toxicological properties of drug candidates. Furthermore, molecular docking has been used as a crucial step for searching possible drug candidates against drug targets. Here we have performed molecular docking studies of some fluorinated sulfonates and their Schiff bases in addition to their ADMET profiles. Additionally, ADMET profiles estimated the solubility of compounds as moderately soluble, and poorly soluble. The intestinal absorption values of the compounds were more than 87% except L28 which showed a value close to RSV with 42.23%. While the distribution properties were estimated by P-gp substrate, BBB permeability and fraction unbound descriptors all the compounds were defined to be non-permeant to CNS. In addition, the metabolism, excretion and toxicity properties of the compounds were estimated. The results revealed that, while L28 was the only compound showing substrate effect for CY2D6 enzyme,

all the compounds were estimated to be substrate for CYP3A4 enzyme. Total clearances of the compounds were found to be in the range of -0.33 ml/min/kg to 1.32 ml/min/kg. In addition, none of the compounds were predicted to have hERG I inhibitory preferences.

All the compounds were placed into binding site of HMG-CoA reductase enzyme alongside with co-crystal RSV drug. While the compounds were docked with calculated RESP charges, the RSV drug was docked with RESP charges and Gasteiger charges. Moreover, eleven compounds showed better binding scores than RSV ligand. The L16 compound showed best binding with a score of -9.43 kcal/mol among studied compounds. The compounds L28 and L15 had close scores to the L16 with the scores of -9.24 kcal/mol and -9.23 kcal/mol, respectively. The interaction analyses showed that compounds form contacts with critical residues of the binding site of enzyme such as Glu559, Asp690, Lys691, Lys692, and Asp767.

Consequently, the study reports that these compounds may inhibit HMG-CoA reductase enzyme and thus can introduce new drug candidates for treatment of cholesterol levels of the human where statins are mostly have been used. For a better understanding of the inhibition effects of the compounds on HMGR, molecular dynamics studies of the compounds complexed with HMGR and binding free energies of the compounds could be performed in the following studies.

References

[1] Bays, H.E., Taub, P.R., Epstein, E., Michos, E.D., Ferraro, R.A., Bailey, A.L., et al., *Ten things to know about ten cardiovascular disease risk factors,* American Journal of Preventive Cardiology, 5, 100149, 2021.

[2] Mullen, P.J., Yu, R., Longo, J., Archer, M.C., & Penn, L.Z., *The interplay between cell signalling and the mevalonate pathway in cancer,* Nature Reviews Cancer, 16(11), 718–731, 2016.

[3] Bennis, F., Favre, G., Legaillard, F., & Soula, G., *Importance of Mevalonate-Derived Products in the Control of Hmg-Coa Reductase-Activity and Growth of Human Lung Adenocarcinoma Cell-Line A549,* International Journal of Cancer, 55(4), 640–645, 1993.

[4] Caruso, M.G., Notarnicola, M., Santillo, M., Cavallini, A., & Di Leo, A., *Enhanced 3-hydroxy-3-methyl-glutaryl coenzyme A reductase activity in human colorectal cancer not expressing low density lipoprotein receptor,* Anticancer Research, 19(1a), 451–454, 1999.

[5] Hawk, M.A., Cesen, K.T., Siglin, J.C., Stoner, G.D., & Ruch, R.J., *Inhibition of lung tumor cell growth in vitro and mouse lung tumor formation by lovastatin,* Cancer Letters, 109(1-2), 217–222, 1996.

[6] Istvan, E.S., Palnitkar, M., Buchanan, S.K., & Deisenhofer, J., *Crystal structure of the catalytic portion of human HMG-CoA reductase: insights into regulation of activity and catalysis,* Embo Journal, 19(5), 819–830, 2000.

[7] Lee, S.J., Ha, M.J., Lee, J., Nguyen, P., Choi, Y.H., Pirnia, F., et al., *Inhibition of the 3-hydroxy-3-methylglutaryl-coenzyme A reductase pathway induces p53-independent*

transcriptional regulation of p21(WAF1/CIP1) in human prostate carcinoma cells, Journal of Biological Chemistry, 273(17), 10618–10623, 1998.

[8] Moorthy, N.S.H.N., Cerqueira, N.M.F.S.A., Ramos, M.J., & Fernandes, P.A., *Ligand based analysis on HMG-CoA reductase inhibitors,* Chemometrics and Intelligent Laboratory Systems, 140, 102–116, 2015.

[9] Grundy, S.M., Cleeman, J.I., Merz, C.N., Brewer, H.B., Jr., Clark, L.T., Hunninghake, D.B., et al., *Implications of recent clinical trials for the National Cholesterol Education Program Adult Treatment Panel III guidelines,* Circulation, 110(2), 227–39, 2004.

[10] Son, M., Baek, A., Sakkiah, S., Park, C., John, S., & Lee, K.W., *Exploration of virtual candidates for human HMG-CoA reductase inhibitors using pharmacophore modeling and molecular dynamics simulations,* PLoS One, 8(12), e83496, 2013.

[11] Pfefferkorn, J.A., Song, Y., Sun, K.L., Miller, S.R., Trivedi, B.K., Choi, C., et al., *Design and synthesis of hepatoselective, pyrrole-based HMG-CoA reductase inhibitors,* Bioorganic & Medicinal Chemistry Letters, 17(16), 4538–4544, 2007.

[12] Silva, M., Philadelpho, B., Santos, J., Souza, V., Souza, C., Santiago, V., et al., *IAF, QGF, and QDF Peptides Exhibit Cholesterol-Lowering Activity through a Statin-like HMG-CoA Reductase Regulation Mechanism: In Silico and In Vitro Approach,* International Journal of Molecular Sciences, 22(20), 2021.

[13] Bose, S., Steussy, C.N., Lopez-Perez, D., Schmidt, T., Kulathunga, S.C., Seleem, M.N., et al., *Targeting Enterococcus faecalis HMG-CoA reductase with a non-statin inhibitor,* Communications Biology, 6(1), 360, 2023.

[14] Marahatha, R., Basnet, S., Bhattarai, B.R., Budhathoki, P., Aryal, B., Adhikari, B., et al., *Potential natural inhibitors of xanthine oxidase and HMG-CoA reductase in cholesterol regulation: in silico analysis,* BMC Complementary Medicine and Therapies, 21(1), 1, 2021.

[15] Aulifa, D.L., Amirah, S.R., Rahayu, D., Megantara, S., & Muchtaridi, M., *Pharmacophore Modeling and Binding Affinity of Secondary Metabolites from Angelica keiskei to HMG Co-A Reductase,* Molecules, 29(13), 2024.

[16] Alameen, A.A., Alothman, M.R., Al Wahibi, M.S., Abdullah, E.M., Ali, R., Abdalla, M., et al., *Potential Effect of Baobab's Polyphenols as Antihyperlipidemic Agents: In Silico Study,* Molecules, 28(16), 2023.

[17] Zhao, Z., Dai, X., Li, C., Wang, X., Tian, J., Feng, Y., et al., *Pyrazolone structural motif in medicinal chemistry: Retrospect and prospect,* European Journal of Medicinal Chemistry, 186, 111893, 2020.

[18] Yoshino, H., *Edaravone for the treatment of amyotrophic lateral sclerosis,* Expert Review of Neurotherapeutics, 19(3), 185–193, 2019.

[19] Meiattini, F., Prencipe, L., Bardelli, F., Giannini, G., & Tarli, P., *The 4-hydroxybenzoate/4-aminophenazone chromogenic system used in the enzymic determination of serum cholesterol,* Clinical Chemistry, 24(12), 2161–5, 1978.

[20] Bussel, J.B., Cheng, G., Saleh, M.N., Psaila, B., Kovaleva, L., Meddeb, B., et al., *Eltrombopag for the treatment of chronic idiopathic thrombocytopenic purpura,* New England Journal of Medicine, 357(22), 2237–47, 2007.

[21] Freitag, F.G., Cady, R., DiSerio, F., Elkind, A., Gallagher, R.M., Goldstein, J., et al., *Comparative study of a combination of isometheptene mucate, dichloralphenazone with acetaminophen and sumatriptan succinate in the treatment of migraine,* Headache, 41(4), 391–8, 2001.

[22] Guo, T., Xia, R., Chen, M., He, J., Su, S., Liu, L., et al., *Biological activity evaluation and action mechanism of chalcone derivatives containing thiophene sulfonate,* RSC Advances, 9(43), 24942–24950, 2019.

[23] Torabi, M., Zolfigol, M.A., Yarie, M., Notash, B., Azizian, S., & Azandaryani, M.M., *Synthesis of triarylpyridines with sulfonate and sulfonamide moieties via a cooperative vinylogous anomeric-based oxidation,* Sci Rep, 11(1), 16846, 2021.

[24] Patel, N.H., Parekh, H.M., & Patel, M.N., *Synthesis, characterization and biological evaluation of manganese(II), cobalt(II), nickel(II), copper(II), and cadmium(II) complexes with monobasic (NO) and neutral (NN) Schiff bases,* Transition Metal Chemistry, 30(1), 13–17, 2005.

[25] Thakor, Y.J., Patel, S.G., & Patel, K.N., *Synthesis, characterization and biocidal studies of some transition metal complexes containing tetra dentate and neutral bi dentate schiff base,* Journal of Chemical and Pharmaceutical Research, 2(5), 518–525, 2010.

[26] Shivakumar, K., Shashidhar, Vithal Reddy, P., & Halli, M.B., *Synthesis, spectral characterization and biological activity of benzofuran Schiff bases with Co(II), Ni(II), Cu(II), Zn(II), Cd(II) and Hg(II) complexes,* Journal of Coordination Chemistry, 61(14), 2274–2287, 2008.

[27] Ramesh, R., Suganthy, P.K., & Natarajan, K., *Synthesis, Spectra and Electrochemistry of Ru(III) Complexes with Tetradentate Schiff Bases,* Synthesis and Reactivity in Inorganic and Metal-Organic Chemistry, 26(1), 47–60, 1996.

[28] Nidhi, S., Rao, D.P., Gautam, A.K., Verma, A., & Gautam, Y., *Schiff bases and their possible therapeutic applications: A review,* Results in Chemistry, 13, 101941, 2025.

[29] Sanyaolu, A., Okorie, C., Marinkovic, A., Haider, N., Abbasi, A.F., Jaferi, U., et al., *The emerging SARS-CoV-2 variants of concern,* Therapeutic Advances in Infectious Disease, 8, 20499361211024372, 2021.

[30] Talele, T.T., Khedkar, S.A., & Rigby, A.C., *Successful Applications of Computer Aided Drug Discovery: Moving Drugs from Concept to the Clinic,* Current Topics in Medicinal Chemistry, 10(1), 127–141, 2010.

[31] Wei, H. & McCammon, J.A., *Structure and dynamics in drug discovery,* npj Drug Discovery, 1(1), 1, 2024.

[32] Guan, L., Yang, H., Cai, Y., Sun, L., Di, P., Li, W., et al., *ADMET-score - a comprehensive scoring function for evaluation of chemical drug-likeness,* Medchemcomm, 10(1), 148–157, 2019.

[33] Sousa, S.F., Ribeiro, A.J., Coimbra, J.T., Neves, R.P., Martins, S.A., Moorthy, N.S., et al., *Protein-ligand docking in the new millennium--a retrospective of 10 years in the field,* Current Medicinal Chemistry, 20(18), 2296–314, 2013.

[34] Niazi, S.K. & Mariam, Z., *Computer-Aided Drug Design and Drug Discovery: A Prospective Analysis,* Pharmaceuticals (Basel), 17(1), 2023.

[35] Istvan, E.S. & Deisenhofer, J., *Structural mechanism for statin inhibition of HMG-CoA reductase,* Science, 292(5519), 1160–4, 2001.

[36] Steussy, C.N., Critchelow, C.J., Schmidt, T., Min, J.K., Wrensford, L.V., Burgner, J.W., 2nd, et al., *A novel role for coenzyme A during hydride transfer in 3-hydroxy-3-methylglutaryl-coenzyme A reductase,* Biochemistry, 52(31), 5195–205, 2013.

[37] Tabernero, L., Bochar, D.A., Rodwell, V.W., & Stauffacher, C.V., *Substrate-induced closure of the flap domain in the ternary complex structures provides insights into the*

mechanism of catalysis by 3-hydroxy-3-methylglutaryl-CoA reductase, Proc Natl Acad Sci U S A, 96(13), 7167–71, 1999.

[38] Istvan, E., *Statin inhibition of HMG-CoA reductase: a 3-dimensional view,* Atherosclerosis Supplements, 4(1), 3–8, 2003.

[39] Holdgate, G.A., Ward, W.H., & McTaggart, F., *Molecular mechanism for inhibition of 3-hydroxy-3-methylglutaryl CoA (HMG-CoA) reductase by rosuvastatin,* Biochemical Society Transactions, 31(Pt 3), 528–31, 2003.

[40] McTaggart, F., Buckett, L., Davidson, R., Holdgate, G., McCormick, A., Schneck, D., et al., *Preclinical and clinical pharmacology of Rosuvastatin, a new 3-hydroxy-3-methylglutaryl coenzyme A reductase inhibitor,* The American Journal of Cardiology, 87(5A), 28B–32B, 2001.

[41] Çakmak, R., Başaran, E., Ercan, S., Boğa, M., Çınar, E., & Topal, G., *Synthesis of new fluorinated sulfonates and their Schiff bases as anti-Alzheimer drug candidates: An in vitro-in silico study,* Journal of Molecular Structure, 1329, 141474, 2025.

[42] Daina, A., Michielin, O., & Zoete, V., *SwissADME: a free web tool to evaluate pharmacokinetics, drug-likeness and medicinal chemistry friendliness of small molecules,* Scientific Reports, 7, 42717, 2017.

[43] Pires, D.E., Blundell, T.L., & Ascher, D.B., *pkCSM: Predicting Small-Molecule Pharmacokinetic and Toxicity Properties Using Graph-Based Signatures,* Journal of Medicinal Chemistry, 58(9), 4066–72, 2015.

[44] Vanquelef, E., Simon, S., Marquant, G., Garcia, E., Klimerak, G., Delepine, J.C., et al., *R.E.D. Server: a web service for deriving RESP and ESP charges and building force field libraries for new molecules and molecular fragments,* Nucleic Acids Research, 39(Web Server issue), W511–7, 2011.

[45] Eberhardt, J., Santos-Martins, D., Tillack, A.F., & Forli, S., *AutoDock Vina 1.2.0: New Docking Methods, Expanded Force Field, and Python Bindings,* Journal of Chemical Information and Modeling, 61(8), 3891–3898, 2021.

[46] Hou, T., *In silico predictions of ADME/T properties: progress and challenge,* Combinatorial Chemistry & High Throughput Screening, 14(5), 306, 2011.

[47] Zhu, J., Wang, J., Yu, H., Li, Y., & Hou, T., *Recent developments of in silico predictions of oral bioavailability,* Combinatorial Chemistry & High Throughput Screening, 14(5), 362–74, 2011.

[48] van de Waterbeemd, H. & Gifford, E., *ADMET in silico modelling: towards prediction paradise?,* Nature Reviews Drug Discovery, 2(3), 192–204, 2003.

[49] Cao, D., Wang, J., Zhou, R., Li, Y., Yu, H., & Hou, T., *ADMET evaluation in drug discovery. 11. PharmacoKinetics Knowledge Base (PKKB): a comprehensive database of pharmacokinetic and toxic properties for drugs,* Journal of Chemical Information and Modeling, 52(5), 1132–7, 2012.

[50] Lipinski, C.A., Lombardo, F., Dominy, B.W., & Feeney, P.J., *Experimental and computational approaches to estimate solubility and permeability in drug discovery and development settings,* Advanced Drug Delivery Reviews, 23(1-3), 3–25, 1997.

[51] Lipinski, C.A., Lombardo, F., Dominy, B.W., & Feeney, P.J., *Experimental and computational approaches to estimate solubility and permeability in drug discovery and development settings,* Advanced Drug Delivery Reviews, 46(1-3), 3–26, 2001.

[52] Ghose, A.K., Viswanadhan, V.N., & Wendoloski, J.J., *A knowledge-based approach in designing combinatorial or medicinal chemistry libraries for drug discovery. 1. A qualitative and quantitative characterization of known drug databases,* Journal of Combinatorial Chemistry, 1(1), 55–68, 1999.

[53] Veber, D.F., Johnson, S.R., Cheng, H.Y., Smith, B.R., Ward, K.W., & Kopple, K.D., *Molecular properties that influence the oral bioavailability of drug candidates,* Journal of Medicinal Chemistry, 45(12), 2615–23, 2002.

[54] Egan, W.J., Merz, K.M., Jr., & Baldwin, J.J., *Prediction of drug absorption using multivariate statistics,* Journal of Medicinal Chemistry, 43(21), 3867–77, 2000.

[55] Muegge, I., Heald, S.L., & Brittelli, D., *Simple selection criteria for drug-like chemical matter,* Journal of Medicinal Chemistry, 44(12), 1841–6, 2001.

[56] Lagorce, D., Douguet, D., Miteva, M.A., & Villoutreix, B.O., *Computational analysis of calculated physicochemical and ADMET properties of protein-protein interaction inhibitors,* Scientific Reports, 7, 46277, 2017.

[57] Duran-Iturbide, N.A., Diaz-Eufracio, B.I., & Medina-Franco, J.L., *In Silico ADME/Tox Profiling of Natural Products: A Focus on BIOFACQUIM,* ACS Omega, 5(26), 16076–16084, 2020.

[58] Malkiewicz, M.A., Szarmach, A., Sabisz, A., Cubala, W.J., Szurowska, E., & Winklewski, P.J., *Blood-brain barrier permeability and physical exercise,* Journal of Neuroinflammation, 16(1), 15, 2019.

[59] Dominguez-Villa, F.X., Duran-Iturbide, N.A., & Avila-Zarraga, J.G., *Synthesis, molecular docking, and in silico ADME/Tox profiling studies of new 1-aryl-5-(3-azidopropyl)indol-4-ones: Potential inhibitors of SARS CoV-2 main protease,* Bioorganic Chemistry, 106, 104497, 2021.

[60] Watanabe, R., Esaki, T., Kawashima, H., Natsume-Kitatani, Y., Nagao, C., Ohashi, R., et al., *Predicting Fraction Unbound in Human Plasma from Chemical Structure: Improved Accuracy in the Low Value Ranges,* Molecular Pharmaceutics, 15(11), 5302–5311, 2018.

[61] Almazroo, O.A., Miah, M.K., & Venkataramanan, R., *Drug Metabolism in the Liver,* Clinical Liver Disease, 21(1), 1–20, 2017.

[62] Zhao, M., Ma, J., Li, M., Zhang, Y., Jiang, B., Zhao, X., et al., *Cytochrome P450 Enzymes and Drug Metabolism in Humans,* International Journal of Molecular Sciences, 22(23), 2021.

[63] Vicki, N., Ari, H., Shabarni, G., Muchtaridi, M., & Tati, H., *Virtual screening campaigns and ADMET evaluation to unlock the potency of flavonoids from Erythrina as 3CLpro SARS-COV-2 inhibitors,* Journal of Applied Pharmaceutical Science, 13(2), 078–088, 2023.

[64] Gesto, D.S., Pereira, C.M.S., Cerqueira, N., & Sousa, S.F., *An Atomic-Level Perspective of HMG-CoA-Reductase: The Target Enzyme to Treat Hypercholesterolemia,* Molecules, 25(17), 2020.

[65] Miziorko, H.M., *Enzymes of the mevalonate pathway of isoprenoid biosynthesis,* Archives of Biochemistry and Biophysics, 505(2), 131–43, 2011.